WILEY | Hindawi

Research Article

Observer-Based Event-Triggered Circle Formation Control for First- and Second-Order Multiagent Systems

Peng Xu [ID],[1] **Guangming Xie** [ID],[1,2,3,4] **Jin Tao** [ID],[5,2] **Minyi Xu** [ID],[1,4] **and Quan Zhou** [ID][5]

[1]*Marine Engineering College, Dalian Maritime University, Dalian 116026, China*
[2]*The State Key Laboratory of Turbulence and Complex Systems, Intelligent Biomimetic Design Lab, College of Engineering, Peking University, Beijing 100871, China*
[3]*Institute of Ocean Research, Peking University, Beijing 100871, China*
[4]*Peng Cheng Laboratory, Shenzhen 518000, China*
[5]*Department of Electrical Engineering and Automation, Aalto University, Espoo 02150, Finland*

Correspondence should be addressed to Jin Tao; jin.tao@aalto.fi and Minyi Xu; xuminyi@dlmu.edu.cn

This paper proposes an observer-based event-triggered algorithm to solve circle formation control problems for both first- and second-order multiagent systems, where the communication topology is modeled by a spanning tree-based directed graph with limited resources. In particular, the observation-based event-triggering mechanism is used to reduce the update frequency of the controller, and the triggering time depends on the norm of the state function and the trigger threshold of measurement errors. The analysis shows that sufficient conditions are established for achieving the desired circle formation, while there exists at least one agent for which the next interevent interval is strictly positive. Numerical simulations of both first- and second-order multiagent systems are also given to demonstrate the effectiveness of the proposed control laws.

1. Introduction

In recent years, many research efforts have been devoted to controlling of multiagent systems (MASs) due to both its practical potentials in a variety of applications [1–3] and theoretical challenges of physical constraints [4–6]. As a significant problem in cooperative control for MASs, formation control, aiming to guide multiple agents to form and maintain predetermined geometries, has attracted considerable interests for its extensive applications in different areas [7–10]. The main focus has been devoted to the design of a distributed formation control framework, especially concerning the robustness against both external disturbances and internal uncertainties [11, 12], as well as the increased number of agents. Moreover, for MASs subjected to aperiodic sampling and communication delays, the problem of cluster formation control was addressed in [10]. Therefore, most existing results on formation control mainly rely on the ideal hypothesis [13–15], e.g., each agent is modeled as having unlimited communication capabilities, unlimited power, and unlimited processing capabilities, which allows arbitrary information to exchange pattern. However, as far as we know, few studies dealt with the limited capacity of communication and the power constraints of agents.

In order to save energy and bandwidth, event-triggered control methods have been presented in [16–20]. One of the most distinct characters of event-triggered control is that control actions only update when specific events occur, which lead to ease the trade-offs among actuator effort, communication, and computation. Moreover, according to the triggered methods, event-triggered control can be mainly divided into state-dependent triggering and time-dependent triggering. A simple state event-triggered schedule based on the feedback control was studied in [16]. The results lead to a guaranteed performance with a fixed sampling rate

requirements concerning the optimizing schedules and sampling rates. In [17], under conditions of decreasing thresholds of the measurement errors exponentially, a time-dependent triggered method was designed to guarantee all agents asymptotic converge to a ball centered at the average consensus. Different from most of the existing fixed threshold parameters, the threshold parameter in the improved event-triggered condition is dynamically adjusted by a dynamic rule in [18]. In [21], by proposing a pull-based event-triggered control strategy, a circle formation control problem for first-order MASs with directed topologies was studied. Further, Wen et al. [22] combined event-triggered protocols to solve circle formation problems of first-order MASs. Also, Wen et al. and Xu et al. [23, 24] have investigated a combination algorithm based on quantized communication technology, where the problem of MASs with a limitation of communication was addressed. Given the above reviews, it is noteworthy to mention that most of the existing results on event-triggered control are to prevent the case of Zeno behavior [25, 26], so that within a finite time interval, an infinite number of samplings generate. Typically, the event trigger interval having a strictly positive lower bound is a sufficient condition to exclude Zeno behavior [27].

Different from previous studies, especially [23], which paid attention to the effect of qualitative communication for event-triggered control, the main objective of this paper is to provide an observer-based event-triggered method to solve circle formation problems for both first- and second-order MASs through a set of directed graphs. In our studies, each agent observes the distance from the counterclockwise direction to its nearest neighbor and the counterpart from the clockwise direction through communication, which is similar to Pioneer 3-DX [28]. In comparison to the literature, we have three main contributions: (i) different from [22] concerning the first-order model, combining with a distributed asynchronous event-triggered control algorithm, a more concise form of the event-triggered condition is designed to solve circle formation problems for both first- and second-order dynamics MASs; (ii) different from taking a complex-coordinate system transformation method in [29], the proposed strategy allows for a reduction of the number of control actions without significantly degrading performance using the simple-coordinate system transformation; and (iii) the resulting asynchronous model achieves the desired equilibrium points asymptotically while at least one agent with a positive next event interval exists, i.e., no trajectory generates in a finite time interval.

The remainder of this paper is organized as follows. Preliminary definitions and problem formulation are given in Section 2. In Section 3, a distributed circle formation control law for first-order MASs and the rigorous analysis of its performance are presented. Section 4 uses the event-triggered rule to address a distributed circle formation problem for second-order MASs. Section 5 discusses the simulation results, and Section 6 concludes the paper.

2. Preliminaries and Problem Formulation

2.1. Preliminaries. Let $\mathbb{R}$ and $\mathbb{R}^{N \times N}$ denote a set of real numbers and a $N \times N$ real matrix, respectively. For a finite set $\mathcal{S}$, let $|\mathcal{S}|$ denote the number of its elements. For a vector or a matrix A, let $\|A\|$, $\|A\|_\infty$, and A^T stand for its Euclidean norm, ∞-norm, and transpose, respectively. Let 1_N and 0_N be the N dimension column vectors with all entries being 1 and 0, respectively. Let a matrix $\text{diag}\{a_1, a_2, \ldots, a_N\}$ represent a diagonal matrix whose diagonal entries are $a_1, a_2, \ldots, a_N$.

Let $\mathcal{G} = (\mathcal{V}, \mathcal{E}, \mathcal{A})$ be a directed graph, in which $\mathcal{V} = \{1, 2, \ldots, N\}$ is a set of nodes, $\mathcal{E} = \mathcal{V} \times \mathcal{V}$ stands for a set of edges, and $\mathcal{A} = [a_{ij}] \in \mathbb{R}^{N \times N}$ denotes a weighted adjacency matrix. In the directed graph $\mathcal{G}$, $(i, i) \notin \mathcal{E}$ for all $i \in \mathcal{V}$, and for edge $(j, i) \in \mathcal{E}$, it starts from node j and ends up with node i. It is known that agent i can perceive state information from agent j. Therefore, agent j is called agent i's in-neighbor. In addition, $\mathcal{N}_i = \{j \in \mathcal{V} \mid (j, i) \in \mathcal{E}\}$ is applied to describe the in-neighbor set of agent i. Particularly, edge (i, j) links with the element a_{ij} of a weighted adjacency matrix $\mathcal{A}$, $a_{ij} > 0$ if and only if $(i, j) \in \mathcal{E}$; otherwise, $a_{ij} = 0$. We use $d_i = \sum_{j=1}^N a_{ij}$ to denote the in-degree of i-th agent and define $\mathcal{L} = \mathcal{D} - \mathcal{A}$ as Laplacian matrix of $\mathcal{G}$, where $\mathcal{D} = \text{diag}\{d_1, d_2, \ldots, d_N\}$. Subsequently, we can list the eigenvalues of $\mathcal{L}$ in a descending order as $\lambda_N \geq \cdots \geq \lambda_2 \geq \lambda_1 = 0$, where λ_N is the spectral radius of $\mathcal{L}$.

We use the two lemmas listed below to facilitate analysis in this paper.

Lemma 1. *For any given $x, y \in \mathbb{R}$ and $a > 0$, the following two properties exist:*

$$xy \leq \frac{a}{2}x^2 + \frac{1}{2a}y^2;$$

$$\left(x^2 + y^2\right) \leq (x + y)^2, \quad \text{if } xy \geq 0. \tag{1}$$

Lemma 2 (see [30]). *Given a directed graph $\mathcal{G}$, which is composed of a spanning tree, a vector $\xi = [\xi_1, \xi_2, \ldots, \xi_N]^T > 0$ satisfies $\sum_{i=1}^N \xi_i = 1$ and $\xi^T \mathcal{L} = 0_N$, where ξ denotes the left eigenvector corresponding to zero eigenvalues of the Laplacian matrix $\mathcal{L}$. Furthermore, $\mathcal{L}^T \Theta + \Theta \mathcal{L}^T$ is semipositive definite, where $\Theta = \text{diag}\{\xi_1, \xi_2, \ldots, \xi_N\}$. After taking square root of each elements of Θ, we get $\Upsilon = \text{diag}\{\gamma_1, \gamma_2, \ldots, \gamma_N\}$; consequently, $\gamma = \sqrt{\xi}$, $i = 1, \ldots, N$.*

Lemma 3 (see [29]). *The linear matrix inequalities*

$$\begin{bmatrix} Q(x) & S(x) \\ S^T(x) & R(x) \end{bmatrix} \geq 0, \tag{2}$$

are equivalent to either one of the conditions listed as below:

$$Q(x) > 0, R(x) - S^T(x)Q^{-1}(x)S(x) \geq 0,$$

$$R(x) > 0, Q(x) - S(x)R^{-1}(x)S^T(x) \geq 0. \tag{3}$$

2.2. Problem Formulation. Given an MAS consisting of N ($N \geq 2$) mobile agents, each agent is initially on a specific circle, and no pair of agents occupies the same position at the same time, as shown in Figure 1. For simplicity, we mark the agents counterclockwise and measure the position of the agent $i, i \in \{1, 2, \ldots, N\}$ at an angle of $x_i(t)$. To be specific, the initial positions of all agents are set to satisfy the condition shown as

$$0 \leq x_1(0) < \cdots < x_i(0) < x_{i+1}(0) < \cdots < x_N(0) < 2\pi. \quad (4)$$

Here, each agent has only two neighbors, that is, in front of or behind it. Let $\mathcal{N}_i = \{i^+, i^-\}$ represent the two neighbors of the mobile agent i, where

$$i^+ = \begin{cases} i + 1, & \text{when } i = 1, 2, \ldots, N - 1, \\ 1, & \text{when } i = N, \end{cases} \quad (5)$$

$$i^- = \begin{cases} i - 1, & \text{when } i = 2, 3, \ldots, N, \\ N, & \text{when } i = 1. \end{cases} \quad (6)$$

The dynamics of agent i are described as

$$\dot{x}_i(t) = u_i(t), \quad i \in \mathcal{V}, \quad (7)$$

where x_i and u_i stand for the scalar state and the control input of agent i, respectively.

Based on counterclockwise at time t, $y_i(t) \in \mathbb{R}$ are presented as the angular distance from agent i to agent i^+. Along with (5) and (6), it yields to

$$y_i(t) = \begin{cases} x_{i^+}(t) - x_i(t) + 2\pi, & \text{when } i = N, \\ x_{i^+}(t) - x_i(t), & \text{when } i = 1, 2, \ldots, N - 1, \end{cases} \quad (8)$$

where $y(t) = [y_1(t), y_2(t), \ldots, y_N(t)]^T \in \mathbb{R}^N$, and $\sum_{i=1}^{N} y_i(t) = 2\pi$ always holds.

Then, define a vector $d = [d_1, d_2, \ldots d_i \ldots, d_N]^T$ to determine a desired circle formation, where $d_i \in \mathbb{R}$ stands for the desired angular distance between agent i and agent i^+. If d satisfies $d_i > 0$ and $\sum_{i=1}^{N} d_i = 2\pi$, the desired circle formation is achievable for MASs.

3. Circle Formation Control for First-Order MASs

In this section, we first give the definition of the circle formation problem for first-order MASs as follows.

Definition 1 (circle formation problem for first-order MASs). Given an admissible circle formation characterized by d, a distributed control law $u_i(t, y_i(t))$, $i = 1, 2, \ldots, N$ can be designed, so that under any initial condition (4), the solution to system (7) converges to the equilibrium point x^*. That is, $y^* = d$.

A way-point control protocol based on sampled date was designed in [8]:

$$u_i(t) = \frac{d_{i^-}}{d_i + d_{i^-}} y_i(t) - \frac{d_i}{d_i + d_{i^-}} y_{i^-}(t), \quad t > 0, i \in \mathcal{V}. \quad (9)$$
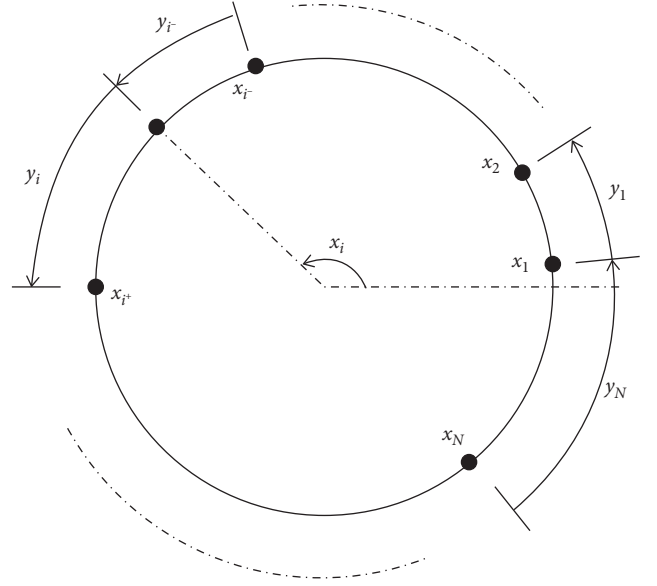

FIGURE 1: Agents distributed on a prescribed circle.

It has been proved that the continuous update control law (9) can move all agents to their equilibrium point x^* but can waste communication bandwidth and unnecessary transmission energy. In order to solve this issue, an observer-based event-triggered circle formation control method for first-order MASs is proposed. It is noteworthy to mention that control actions of each agent only update at the event-triggered sampling instants, where continuous communication between neighboring agents is maintained. Here, we use an increasing sequence $(t_0^i, t_1^i, \ldots, t_k^i, \ldots)$ to represent the event instants of agent i, such that the state of agent i at the kth event instant is described as $y_i(t_k^i)$. Note that each agent has its own event sequence since all agents are triggered asynchronously.

According to event-triggered strategies, we design the distributed circle formation control law for agent i as

$$u_i(t) = \frac{d_{i^-}}{d_{i^-} + d_i} y_i(t_k^i) - \frac{d_i}{d_{i^-} + d_i} y_{i^-}(t_k^{i^-}), \quad t \in [t_k^i, t_{k+1}^i), \quad (10)$$

where $t_k^{i^-} \triangleq \text{argmin}_{l \in \mathbb{N}, t \geq t_l^{i^-}} \{t - t_l^{i^-}\}$ represents the last event instant of agent i^- and $y_i(t_k^i)$ denotes the observer angular distance.

From (10), agent i's controller only updates at its own event sequence $(t_0^i, t_1^i, \ldots, t_k^i, \ldots)$. For simplicity, let $\widehat{y}_i(t) = y_i(t_k^i)$; consequently, the control law (10) can be represented as

$$u_i(t) = \frac{d_i d_{i^-}}{d_{i^-} + d_i} \left(\widehat{\delta}_i(t) - \widehat{\delta}_{i^-}(t) \right), \quad t \in [t_k^i, t_{k+1}^i), \quad (11)$$

where $\widehat{\delta}_i(t) = \widehat{y}_i(t)/d_i$, $\widehat{\delta}_{i^-}(t) = \widehat{y}_{i^-}(t)/d_i$.

Replacing (2) and (5) into (7), the closed-loop form of agent i is rearranged by using δ_i as

$$\dot{\delta}_i(t) = \sum_{j \in \mathcal{N}_i} \frac{d_j}{d_i + d_j} \left(\hat{\delta}_j(t) - \hat{\delta}_i(t) \right), \quad t \geq 0. \quad (12)$$

Define $e_i(t) = \hat{\delta}_i(t) - \delta_i(t)$; then, a compact form of system dynamics is

$$\dot{\delta}(t) = -L_d^T(\delta(t) + e(t)), t \in \left[t_k^i, t_{k+1}^i\right), \quad (13)$$

where $\delta(t) = [\delta_1(t), \delta_2(t), \ldots, \delta_N(t)] \in \mathbb{R}^N,$ $e(t) = [e_1(t), e_2(t), \ldots, e_N(t)] \in \mathbb{R}^N,$ and

$$L_d = \begin{bmatrix} \frac{d_2}{d_2 + d_1} + \frac{d_N}{d_N + d_1} & -\frac{d_1}{d_2 + d_1} & \cdots & 0 & -\frac{d_1}{d_N + d_1} \\ -\frac{d_2}{d_2 + d_1} & \frac{d_3}{d_3 + d_2} + \frac{d_1}{d_2 + d_1} & \cdots & 0 & 0 \\ \vdots & \vdots & \vdots & \vdots & \vdots \\ 0 & 0 & \cdots & \frac{d_N}{d_N + d_{N-1}} + \frac{d_{N-2}}{d_{N-1} + d_{N-2}} & -\frac{d_{N-1}}{d_N + d_{N-1}} \\ -\frac{d_N}{d_N + d_1} & 0 & \cdots & -\frac{d_N}{d_N + d_{N-1}} & \frac{d_1}{d_N + d_1} + \frac{d_{N-1}}{d_N + d_{N-1}} \end{bmatrix}. \quad (14)$$

According to the control law (5) and MAS (1), the circle formation control for first-order MASs is solvable by Theorem 1.

Theorem 1. *For any admissible circle formation characterized by d, considering system (7) and the designed control law (5) on the digraph $\mathcal{G}$, the circle formation problem can be solved when the event-triggered condition is designed as*

$$f_i(t) = \|e_i(t)\| - \frac{\sigma \|\gamma_i \overline{\delta}_i\|}{\|\Upsilon L_d^T\|}, \quad 0 < \sigma < 1, \quad (15)$$

where $\overline{\delta}_i$ is the ith elements of $\overline{\delta} = [\overline{\delta}_1, \overline{\delta}_2, \ldots, \overline{\delta}_N]^T \triangleq L_d^T \delta$, Υ is the same diagonal matrix as in Lemma 2, and γ_i is the ith diagonal element of matrix Υ. Moreover, in system (7), there exists at least one agent $m \in \mathcal{V}$ that the next interevent interval is strictly positive under the event-triggered condition (15).

Proof. A Lyapunov function candidate is taken into consideration

$$V(t) = \frac{1}{4}\delta^T(t)\left(L_d\Theta + \Theta L_d^T\right)\delta(t), \quad (16)$$

where Θ is the same diagonal matrix as Lemma 2, such that $L_d\Theta + \Theta L_d^T$ is semipositive definite.

Accordingly, $\dot{V}(t) \leq 0$ and $\dot{V}(t) = 0$ if and only if the circle formation problem can be solved. The derivative of the Lyapunov function (16) along trajectories of the system is derived as

$$\begin{aligned} \dot{V}(t) &= \delta^T(t)L_d\Theta\left(-L_d^T(\delta(t) + e(t))\right) \\ &= -\delta^T(t)L_d\Theta L_d^T\delta(t) - \delta^T(t)L_d\Theta L_d^T e(t) \quad (17) \\ &\leq -\left\|\Upsilon L_d^T\delta(t)\right\|^2 + \left\|\Upsilon L_d^T\delta(t)\right\|\left\|\Upsilon L_d^T e(t)\right\|. \end{aligned}$$

After enforcing the event condition (15), we get $\|\Upsilon L_d^T e(t)\| \leq \|\Upsilon L_d^T\|\|e(t)\| \leq \sigma\|\Upsilon L_d^T\delta\|$. Thus, (17) is rewritten as

$$\begin{aligned} \dot{V}(t) &\leq \left\|\Upsilon L_d^T\delta(t)\right\|^2(\sigma - 1) \\ &\leq \left\|\Upsilon\overline{\delta}(t)\right\|^2(\sigma - 1). \end{aligned} \quad (18)$$

Because $0 < \sigma < 1$, we can get $\dot{V}(t) \leq 0$ and $\dot{V}(t) = 0$ if and only if the circle formation problem can be solved.

Next, we explain the achievement of the circle formation in detail. According to the Lemma 2, we get

$$\sum_{i=1}^N \xi_i\delta_i(t+1) = \sum_{i=1}^N \xi_i\delta_i(t) = \cdots = \sum_{i=1}^N \xi_i\delta_i(0). \quad (19)$$

Combining (10) and (15), all conditions result in $\lim_{t\to\infty}\delta_i(t) = \lim_{t\to\infty}\delta_j(t) = \sum_{i=1}^N \xi_i\delta_i(0) = c$, where $c \in \mathbb{R}$ remains constant. In addition, $\sum_{i=1}^N y_i = 2\pi, \forall t \geq 0$ always satisfies and $\sum_{i=1}^N d_i = 2\pi$. Together with $y_i(t) = d_i\delta_i(t)$, we obtain $c = 1$. More exactly, $\lim_{t\to\infty}y(t) = d$, which indicates that the designed circle formation can be solved in first-order MASs.

For agent i, the period $\|e_i(t)\|/\gamma_i\overline{\delta}_i$, increasing from 0 to $\sigma/\|\Upsilon L_d^T\|$, is regarded as the event interval between t_{k+1}^i and t_k^i. Define $m = \text{argmax}_{i \in \mathcal{V}}\|\gamma_i\overline{\delta}_i\|$; therefore, agent m stands for the maximum norm of $\gamma_i\overline{\delta}_i$ among all the agents, which implies

$$\frac{\|e_m(t)\|}{\|\gamma_m\overline{\delta}_m\|} \le \frac{\|e(t)\|}{\|\gamma_m\overline{\delta}_m\|} \le \frac{\sqrt{N}\|e(t)\|}{\|\Upsilon\overline{\delta}\|}. \tag{20}$$

From (20), the time $\|e_m(t)\|/\|\gamma_m\overline{\delta}_m\|$ attaining $\sigma/\|\Upsilon L_d^T\|$ is longer than $\sqrt{N}\|e(t)\|/\|\Upsilon\overline{\delta}\|$. That is, $\tau_m > \tau$, where τ_m represents positive interval $(t_{k+1}^m - t_k^m)$ lower bound and τ is the time $e(t)/\Upsilon\overline{\delta}$ increasing from 0 to $\sigma/\sqrt{N}\|\Upsilon L_d^T\|$. Thereby, the time derivative of $\|e(t)\|/\|\Upsilon\overline{\delta}\|$ is

$$\begin{aligned}
\frac{d}{dt}\frac{\|e(t)\|}{\|\Upsilon\overline{\delta}\|} &= \frac{d}{dt}\frac{\left(e(t)^T e(t)\right)^{1/2}}{\left(\overline{\delta}^T\Upsilon\Upsilon\overline{\delta}\right)^{1/2}} = \frac{e(t)\dot{e}(t)}{\|e(t)\|\|\Upsilon\overline{\delta}\|} \\
&\quad - \frac{\overline{\delta}^T\Upsilon\Upsilon\dot{\overline{\delta}}\|e(t)\|}{\|\Upsilon\overline{\delta}\|^3} \\
&= \frac{-e(t)\Upsilon^{-1}\Upsilon\left(\overline{\delta} + L_d^T e(t)\right)}{\|e(t)\|\|\Upsilon\overline{\delta}\|} \\
&\quad - \frac{\overline{\delta}^T\Upsilon\Upsilon L_d^T\left(\overline{\delta} + L_d^T e(t)\right)\|e(t)\|}{\left\|\Upsilon\overline{\delta}\right\|^2\|\Upsilon\overline{\delta}\|} \\
&\le \frac{\|\Upsilon^{-1}\|\left(\|\Upsilon\overline{\delta}\| + \|\Upsilon L_d^T e(t)\|\right)}{\|\Upsilon\overline{\delta}\|} \\
&\quad + \frac{\|\Upsilon L_d^T\|\|\Upsilon^{-1}\|\left(\|\Upsilon\overline{\delta}\| + \|\Upsilon L_d^T e(t)\|\right)\|e(t)\|}{\|\Upsilon\overline{\delta}\|^2} \\
&\le \|\Upsilon\|\left(1 + \frac{\|e(t)\|\|\Upsilon L_d^T\|\|\Upsilon\overline{\delta}\|}{\|\Upsilon\overline{\delta}\|}\right)^2.
\end{aligned} \tag{21}$$

Using β to replace $\|e(t)\|/\|\Upsilon\overline{\delta}\|$, it yields to $\dot{\beta} \le \|\Upsilon^{-1}\|(1 + \|\Upsilon L_d^T\|\beta)^2$. Here, $\beta \le \alpha(t,\alpha_0)$, where $\alpha(t,\alpha_0)$ is the solution of $\dot{\alpha}(t,\alpha_0) = \|\Upsilon^{-1}\|(1 + \|\Upsilon L_d^T\|\alpha(t,\alpha_0))^2$, $\alpha(0,\alpha_0) = \alpha_0$. According to

$$\frac{d\alpha}{\|\Upsilon^{-1}\|\left(1 + \|\Upsilon L_d^T\|\alpha(t,\alpha_0)\right)^2} = dt, \tag{22}$$

we know that there exists the interval t which satisfies $\alpha(\tau,0) = \sigma/\|\Upsilon L_d^T\|$, such that the event interval between instants t_k and t_{k+1} is lower bounded. By solving the difference equation (22), it yields to

$$\begin{aligned}
\tau &= \frac{d\alpha(\tau,0)}{\|\Upsilon^{-1}\|\left(1 + \|\Upsilon L_d^T\|\alpha(\tau,0)\right)} \\
&= \frac{\sigma}{(1+\sigma)\|\Upsilon L_d^T\|\|\Upsilon^{-1}\|}.
\end{aligned} \tag{23}$$

Calculated from (23), we obtain $\tau = \sigma/((\sqrt{N}+\sigma)\|\Upsilon L_d^T\|\|\Upsilon^{-1}\|)$, where τ is the time $\|e(t)\|/\|\Upsilon\overline{\delta}\|$ from 0 to $\sigma/(\sqrt{N}\|\Upsilon L_d^T\|)$, which derives to agent m' lower bound of interval between two event instants:

$$\tau_m = \frac{\sigma}{(\sqrt{N}+\sigma)\|\Upsilon L_d^T\|\|\Upsilon^{-1}\|}. \tag{24}$$

From $\tau_m > 0$, we conclude that in system (7), there exists at least one agent $m \in \mathcal{V}$, the next interevent interval of which is strictly positive under event-triggered condition (15). □

4. Circle Formation Control for Second-Order MASs

Given a second-order MAS with N agents

$$\begin{cases}
\dot{v}_i(t) = u_i(t), \\
\dot{x}_i(t) = v_i(t), \quad i = 1, 2, \dots, N,
\end{cases} \tag{25}$$

where $x_i \in \mathbb{R}$ is the angular state of agent i, $v_i(t) \in \mathbb{R}$ is its angular velocity state, and $u_i \in \mathbb{R}$ denotes its control input.

Similar to transformation of (8), we obtain

$$\zeta_i(t) = v_{i+}(t) - v_i(t), \quad i = 1, 2, \dots, N, \tag{26}$$

where $\zeta(t) = [\zeta_1(t), \zeta_2(t), \dots, \zeta_N(t)] \in \mathbb{R}^N$ and $\sum_{i=1}^N \zeta_i = 0$ always holds.

The definition of the circle formation problem for second-order MASs is described as follows.

Definition 2 (circle formation problem for second-order MASs). Considering an admissible circle formation, which is characterized by d, we can design a distributed control law $u_i(t, y_i(t), \zeta_i(t)), i = 1, 2, \dots, N$, such that the solution to system (25) converges to the equilibrium points x^* under any initial condition (4). Namely, $y^* = d$ and $\zeta = 0_N$ are satisfied.

Let $\widehat{\zeta}_i(t) = \zeta_i(t_k^i)$ and $\widehat{\zeta}_{i-} = \zeta_{i-}(t_k^{i-})$ stand for the observer angular velocity distance of agent i and $i-$, respectively. From [8], the control law for agent i can be designed as

$$\begin{aligned}
u_i(t) &= \frac{d_{i-}}{d_i + d_{i-}}\varphi\left(\widehat{y}_i(t) + \widehat{\zeta}_i(t)\right) \\
&\quad - \frac{d_i}{d_i + d_{i-}}\varphi\left(\widehat{y}_{i-}(t) + \widehat{\zeta}_{i-}(t)\right), \quad i = 1, 2, \dots N,
\end{aligned} \tag{27}$$

where $\widehat{\zeta}_i(t) = \zeta_i(t_k^i)$, $\widehat{\zeta}_{i-} = \zeta_{i-}(t_k^{i-})$ and the positive control gain φ is determined in sequel.

For simplicity, we have

$$\begin{aligned}
e_{i,y}(t) &= \widehat{y}_i(t) - y_i(t), \\
e_{i,\zeta}(t) &= \widehat{\zeta}_i(t) - \zeta_i(t), \\
t &\in \left[t_k^i, t_{k+1}^i\right).
\end{aligned} \tag{28}$$

Substituting (8), (26), and (27) into (25), the closed-loop system is written as

$$\begin{bmatrix} \dot{y}(t) \\ \dot{\zeta}(t) \end{bmatrix} = \begin{bmatrix} 0 & I_N \\ -\varphi L_d & -\varphi L_d \end{bmatrix} \begin{bmatrix} y(t) \\ \zeta(t) \end{bmatrix} + \begin{bmatrix} 0 & 0 \\ -\varphi L_d & -\varphi L_d \end{bmatrix} \begin{bmatrix} e_y(t) \\ e_\zeta(t) \end{bmatrix},$$

(29)

where $e_y(t) = [e_{1,y}(t), e_{2,y}(t), \ldots, e_{N,y}(t)] \in \mathbb{R}^N$, $e_\zeta(t) = [e_{1,\zeta}(t), e_{2,\zeta}(t), \ldots, e_{N,\zeta}(t)] \in \mathbb{R}^N$, and L_d is the same matrix as in (14).

Define $D = \mathrm{diag}\{d_1, d_2, \ldots, d_N\}$; we then have the coordinate transformation as

$$\delta(t) = D^{-1} y(t),$$
$$\theta(t) = D^{-1} \zeta(t),$$
$$e_1(t) = D^{-1} e_y(t),$$
$$e_2(t) = D^{-1} e_\zeta(t).$$

(30)

Consequently, system (29) is rearranged as

$$\begin{bmatrix} \dot{\delta}(t) \\ \dot{\theta}(t) \end{bmatrix} = \begin{bmatrix} 0 & I_N \\ -\varphi L_d^T & -\varphi L_d^T \end{bmatrix} \begin{bmatrix} \delta(t) \\ \theta(t) \end{bmatrix} + \begin{bmatrix} 0 & 0 \\ -\varphi L_d^T & -\varphi L_d^T \end{bmatrix} \begin{bmatrix} e_1(t) \\ e_2(t) \end{bmatrix}.$$

(31)

Giving $\omega(t) = [\delta^T(t), \theta^T(t)]^T$ and $\hat{e}(t) = [e_1^T(t), e_2^T(t)]^T$, system (31) can be rewritten as

$$\dot{\omega}(t) = \begin{bmatrix} 0 & I_N \\ -\varphi L_d^T & -\varphi L_d^T \end{bmatrix} \omega(t) + \begin{bmatrix} 0 & 0 \\ -\varphi L_d^T & -\varphi L_d^T \end{bmatrix} \hat{e}(t).$$

(32)

Before designing any event-triggered conditions, the Lyapunov function candidate is given as

$$V(t) = \frac{1}{2} \omega^T(t) \begin{bmatrix} r L_d \Theta L_d^T & k_1 L_d \Theta \\ \\ k_1 \Theta L_d^T & \frac{1}{2} \nu (L_d \Theta + \Theta L_d^T) \end{bmatrix} \omega(t),$$

(33)

where r, k_1, and ν are positive constants.

Theorem 2. *The Lyapunov function (33) satisfies system (25) when the condition*

$$r \geq \frac{2 k_1^2}{o \nu} \xi_{\max},$$

(34)

holds simultaneously, where $\xi_{\max}$ is considered as the maximum element of vector ξ in Lemma 2 and o denotes a positive constant.

Proof. When the Lyapunov function equals to zero, the circle formation problem can be solved. In this case, the circle formation cannot be achieved. According to (33), it yields to

$$2V(t) = r \delta^T(t) L_d \Theta L_d^T \delta(t) + k_1 \delta^T(t) L_d \Theta \theta(t)$$
$$+ k_1 \theta^T(t) \Theta L_d^T \delta(t) + \theta^T(t) \frac{1}{2} \nu (L_d \Theta + \Theta L_d^T) \theta(t).$$

(35)

From $\bar{\delta}(t)$ and Lemma 2, we can observe that the desired circle formation is achieved by $r \bar{\delta}^T(t) L_d \Theta L_d^T \delta(t) = r \bar{\delta}^T(t) \Theta \bar{\delta}(t) = r \sum_{i=1}^N \xi_i \|\bar{\delta}_i(t)\|^2 = 0$, $\theta^T(t) 1/2 \nu (L_d \Theta + \Theta L_d^T) \theta(t) = 0$ and semipositive definite matrix $1/2 \nu (L_d \Theta + \Theta L_d^T) \nu$.

We define a positive constant o as

$$o \triangleq \min_{L_d^T \theta \neq 0, \theta \neq 0} \frac{\theta^T(t) (L_d \Theta + \Theta L_d^T) \theta(t)}{\theta^T(t) \theta(t)}.$$

(36)

Since $L_d \Theta + \Theta L_d^T$ can be taken as positive (semipositive) definite with a single zero eigenvalue, there exists a unitary matrix $P = [p_1, p_2, \ldots, p_N] \in \mathbb{R}^{N \times N}$ such that $L_d \Theta + \Theta L_d^T = PSP^T$, where S denotes diagonal matrix with $\mathrm{diag}\{s_1, s_2, \ldots, s_N\}$. In addition, s_i is the eigenvalue of $L_d \Theta + \Theta L_d^T$ associated with eigenvector p_i. Note that assuming $s_1 = 0$, the corresponding eigenvector $p_1 = 1_N$. By defining $\varsigma = [\varsigma_1, \varsigma_2, \ldots, \varsigma_N] \triangleq P^T \theta(t)$, we get

$$o = \min_{L_d^T \theta \neq 0, \theta \neq 0} \theta^T(t) (L_d \Theta + \Theta L_d^T) \theta(t)$$
$$= \min_{L_d^T \theta \neq 0, \theta \neq 0} \theta^T(t) PSP^T \theta(t)$$
$$= \min_{L_d^T \theta \neq 0, \theta \neq 0} \varsigma^T S \varsigma$$
$$= \min_{L_d^T \theta \neq 0, \theta \neq 0} \sum_{i=1}^N s_i \varsigma_i^2 \geq 0.$$

(37)

From (37), we observe that $o = 0$ if and only if $L_d^T P \varsigma \neq 0$, $\varsigma^T \varsigma = 1$ and $\varsigma_2 = \cdots = \varsigma_N = 0$, which indicates that $\varsigma_1 = 1$ or $\varsigma_1 = -1$. Without loss of generality, $\varsigma_1 = 1$ can be used for further analysis. In that case, we have $L_d^T P \varsigma = L_d^T [p_1, p_2, \ldots, p_N][1, 0, \ldots, 0]^T = L_d^T p_1 = L_d^T 1_N = 0$, which violates the assumptions $L_d^T P \varsigma \neq 0$. Thus, $o > 0$ when the circle formation is not achieved. From o, we conclude that $o \theta^T(t) \theta(t) \leq \theta^T(t) (L_d \Theta + \Theta L_d^T) \theta(t)$. Therefore, we have

$$V(t) \geq \frac{1}{2} \omega^T(t) \begin{bmatrix} r L_d \Theta L_d^T & k_1 L_d \Theta \\ \\ k_1 \Theta L_d^T & \frac{1}{2} \nu o \end{bmatrix} \omega(t).$$

(38)

Also, according to Lemma 3, $(1/2) \omega^T(t) \begin{bmatrix} r L_d \Theta L_d^T & k_1 L_d \Theta \\ k_1 \Theta L_d^T & (1/2) \nu o \end{bmatrix} \omega(t)$ is semipositive definite when $(1/2) \nu o > 0$ and

$$r L_d \Theta L_d^T - r L_d \Theta L_d^T \left(\frac{1}{2} \nu o\right)^{-1} k_1 \Theta L_d^T$$
$$= L_d \Theta L_d^T r - L_d \left(\frac{2 k_1^2}{o \nu} \Theta^2\right) L_d^T \geq 0.$$

(39)

From (39), we draw a conclusion that $r \geq (2 k_1^2 / o \nu) \xi_i$. The Lyapunov function (33) is semipositive definite and if the circle formation problem is solvable, it equals to 0. Therefore, this candidate Lyapunov function (33) satisfies the second-order MAS (25). $\square$

Theorem 3. *For any admissible circle formation characterized by d, taking into account system (25) and the designed control law (27) over the digraph $\mathcal{G}$, the circle formation problem can be solved when the event-triggered condition is designed as*

$$f_i(t) = \frac{\varphi \left\| \Upsilon L_d^T \right\|^2 (k_1 + \nu)}{2k} \left(\left\| e_1^i(t) \right\|^2 + \left\| e_2^i(t) \right\|^2 \right)$$
$$- \sigma(\varphi k_1 - \varphi k k_1) \left\| \tilde{\delta}_i(t) \right\|^2 \qquad (40)$$
$$- \sigma(\varphi \nu - k_2 - \varphi k \nu) \left\| \tilde{\theta}_i(t) \right\|^2,$$

where $0 < \sigma < 1$, k, k_1, k_2, and ν stand for positive constants and $\tilde{\delta}_i(t)$ and $\tilde{\theta}_i(t)$ are the i-th element of vector $\tilde{\delta}(t)$ and $\tilde{\theta}(t)$, respectively.

Let $[\tilde{\delta}^T(t) \tilde{\theta}^T(t)]^T = (I_2 \otimes \Upsilon)[\bar{\delta}^T(t) \bar{\theta}^T(t)]^T$ and the conditions

$$\varphi k_1 - \varphi k k_1 > 0,$$
$$\varphi \nu - k_2 - \varphi k \nu > 0, \qquad (41)$$

hold simultaneously; there exists at least one agent $g \in \mathcal{N}$ for which the next interevent interval is strictly positive under the event-triggered condition (40) in system (25).

Proof. By combining (33) and (36), we have

$$V(t) = \frac{1}{2} \omega^T(t) \begin{bmatrix} r L_d \Theta L_d^T & k_1 L_d \Theta \\ k_1 \Theta L_d^T & \frac{1}{2} \nu (L_d \Theta + \Theta L_d^T) \end{bmatrix} \omega(t)$$
$$= \frac{1}{2} \omega^T(t) \begin{bmatrix} r L_d \Theta L_d^T & k_1 L_d \Theta \\ k_1 \Theta L_d^T & \nu L_d \Theta \end{bmatrix} \omega(t). \qquad (42)$$

$\square$

Taking time derivative of Lyapunov function (33) along all trajectories of system (29), we get

$$\dot{V}(t) = \frac{1}{2} \omega^T(t) \begin{bmatrix} r L_d \Theta L_d^T & k_1 L_d \Theta \\ k_1 \Theta L_d^T & \nu L_d \Theta \end{bmatrix} \dot{\omega}(t)$$
$$= \omega^T(t) \begin{bmatrix} r L_d \Theta L_d^T & k_1 L_d \Theta \\ k_1 \Theta L_d^T & \nu L_d \Theta \end{bmatrix}$$
$$\times \left(\begin{bmatrix} 0 & I_N \\ -\varphi L_d^T & -\varphi L_d^T \end{bmatrix} \omega(t) + \begin{bmatrix} 0 & 0 \\ -\varphi L_d^T & -\varphi L_d^T \end{bmatrix} \hat{e}(t) \right)$$
$$= \omega^T(t) \begin{bmatrix} -\varphi k_1 L_d \Theta L_d^T & r L_d \Theta L_d^T - \varphi k_1 L_d \Theta L_d^T \\ -\varphi \nu L_d \Theta L_d^T & k_1 \Theta L_d^T - \varphi \nu L_d \Theta L_d^T \end{bmatrix} \omega(t)$$
$$+ \omega^T(t) \begin{bmatrix} r L_d \Theta L_d^T & k_1 L_d \Theta \\ k_1 \Theta L_d^T & \nu L_d \Theta \end{bmatrix} \begin{bmatrix} 0 & 0 \\ -\varphi L_d^T & -\varphi L_d^T \end{bmatrix} \hat{e}(t). \qquad (43)$$

Then, (43) can be classified into two parts. The former part of (43) is computed by

$$\omega^T(t) \begin{bmatrix} -\varphi k_1 L_d \Theta L_d^T & r L_d \Theta L_d^T - \varphi k_1 L_d \Theta L_d^T \\ -\varphi \nu L_d \Theta L_d^T & k_1 \Theta L_d^T - \varphi \nu L_d \Theta L_d^T \end{bmatrix} \omega(t)$$
$$= -\varphi k_1 \delta^T(t) L_d \Theta L_d^T \delta(t) + k_1 \theta^T(t) \Theta L_d^T \theta(t)$$
$$- \varphi \nu \theta^T(t) L_d \Theta L_d^T \theta(t) + \delta^T(t)(r - \varphi k_1 - \varphi \nu) L_d \Theta L_d^T \theta(t). \qquad (44)$$

By $r = \varphi(k_1 - \nu)$ and condition (41) and (44) implies

$$- \varphi k_1 \delta^T(t) L_d \Theta L_d^T \delta(t) + k_1 \theta^T(t) \Theta L_d^T \theta(t)$$
$$- \varphi \nu \theta^T(t) L_d \Theta L_d^T \theta(t)$$
$$+ \delta^T(t)(r - \varphi k_1 - \varphi \nu) L_d \Theta L_d^T \theta(t)$$
$$\leq - \varphi k_1 \delta^T(t) L_d \Theta L_d^T \delta(t) - (\varphi \nu - k_2) \theta^T(t) \Theta L_d \Theta L_d^T \theta(t). \qquad (45)$$

According to Lemma 1, the latter part of (43) is rearranged into

$$\omega^T(t) \begin{bmatrix} r L_d \Theta L_d^T & k_1 L_d \Theta \\ k_1 \Theta L_d^T & \nu L_d \Theta \end{bmatrix} \begin{bmatrix} 0 & 0 \\ -\varphi L_d^T & -\varphi L_d^T \end{bmatrix} \hat{e}(t)$$
$$\leq \varphi k_1 \left\| \delta^T(t) L_d \Theta L_d^T e_1(t) \right\| + \varphi k_1 \left\| \delta^T(t) L_d \Theta L_d^T e_2(t) \right\|$$
$$+ \varphi \nu \left\| \theta^T(t) L_d \Theta L_d^T e_1(t) \right\| + \varphi \nu \left\| \theta^T(t) L_d \Theta L_d^T e_2(t) \right\|$$
$$= \varphi k_1 \left\| \tilde{\delta}^T(t) \Upsilon L_d^T e_1(t) \right\| + \varphi k_1 \left\| \tilde{\delta}^T(t) \Upsilon L_d^T e_2(t) \right\| \qquad (46)$$
$$+ \varphi \nu \left\| \tilde{\theta}^T(t) \Upsilon L_d^T e_1(t) \right\| + \varphi \nu \left\| \tilde{\theta}^T(t) \Upsilon L_d^T e_2(t) \right\|$$
$$\leq k k_1 \varphi \left\| \tilde{\delta}(t)^2 \right\| + k \nu \varphi \left\| \tilde{\theta}(t) \right\|^2$$
$$+ \frac{\varphi(k_1 + \nu) \left\| \Upsilon L_d^T \right\|^2}{2k} \left(\left\| e_1(t) \right\|^2 + \left\| e_2(t) \right\|^2 \right).$$

Combining (45) and (46), (43) can be written as

$$\dot{V}(t) \leq (-\varphi k_1 + k k_1 \varphi) \left\| \tilde{\delta}(t) \right\|^2 + (-\varphi \nu + k \nu \varphi) \left\| \tilde{\theta}(t) \right\|^2$$
$$+ \frac{\varphi(k_1 + \nu) \left\| \Upsilon L_d^T \right\|^2}{2k} \left(\left\| e_1(t) \right\|^2 + \left\| e_2(t) \right\|^2 \right). \qquad (47)$$

In view of the event-triggered function (40) satisfying $f_i(t) < 0$, we conclude that

$$\frac{\varphi \left\| \Upsilon L_d^T \right\|^2 (k_1 + \nu)}{2k} \left(\left\| e_1(t) \right\|^2 + \left\| e_2(t) \right\|^2 \leq \sigma(\varphi k_1 - \varphi k k_1) \left\| \tilde{\delta}(t) \right\|^2 \right)$$
$$+ \sigma(\varphi \nu - k_2 - \varphi k \nu) \left\| \tilde{\theta}(t) \right\|^2. \qquad (48)$$

From (48), we summarize that the Lyapunov function (33) is negative unless the circle formation for the second-order MAS is achievable. Moreover, we have $\tilde{\omega}_{t \to \infty}(t) = 0$, that is $\tilde{\delta}_{t \to \infty}(t) = 0$ and $\tilde{\theta}_{t \to \infty}(t) = 0$. Thus, we get

$\lim_{t \to \infty} \delta_i(t) = \lim_{t \to \infty} \delta_j(t) = c$, $\lim_{t \to \infty} \theta_i(t) = \lim_{t \to \infty} \theta_j(t) = l$, $c, l \in \mathbb{R}$. Note that $y(t) = D\delta(t)$ and $\zeta(t) = D\theta(t)$. Then, $\sum_{i=1}^{N} y_i = 2\pi$, $\sum_{i=1}^{N} \zeta_i = 0$, $\forall t \geq 0$ always satisfies and $\sum_{i=1}^{N} d_i = 2\pi$. We conclude that $c = 1$, $l = 0$. To be more precise, $\lim_{t \to \infty} y(t) = d$, and $\lim_{t \to \infty} \zeta(t) = 0$.

The result shows that the circle formation can be achieved by all mobile agents. Furthermore, we illustrate the interevent times $(t^i_{k+1} - t^i_k)$ are positive lower bounded.

Using event-triggered condition (40), we obtain that the interval $(t^i_{k+1} - t^i_k)$ is the time $((\varphi \| \Upsilon L_d^T \|^2 (k_1 + \nu))/2k)(\|e^i_1(t)\|^2 + \|e^i_2(t)\|^2)$ that increases from 0 to $-\sigma(\varphi k_1 - \varphi k k_1)\|\tilde{\delta}_i(t)\|^2 - \sigma(\varphi \nu - k_2 - \varphi k \nu)\|\tilde{\theta}_i(t)\|^2$.

Here, we use τ_i to represent the interval. Then, τ_i is longer or equal to the time $((\|\Upsilon L_d^T\|(k_1 + \nu))/2k)\varphi(\|e^i_1(t)\|^2 + \|e^i_2(t)\|^2)$ increasing from 0 to

$\sigma \mu_{\min}(\|\tilde{\delta}_i(t)\|^2 + \|\tilde{\theta}_i(t)\|^2)$, where $\mu_{\min} = \min\{\varphi k_1 - \varphi k k_1, \varphi \nu - k_2 - \varphi k \nu\}$.

Let $\hat{\tau}_i$ denote the time $(\|e^i_1(t)\|^2 + \|e^i_2(t)\|^2)/(\|\tilde{\delta}_i(t)\|^2 + \|\tilde{\theta}_i(t)\|^2)$ from 0 $to 2\sigma k \mu_{\min}/((k_1 + \nu)\varphi \|\Upsilon L_d^T\|)$. From the analysis, the $k + 1$-th event of agent i occurs after the time $t^i_k + \hat{\tau}_i$. Similar to the definition of m, we define $g = \text{argmax}_{i \in \mathcal{V}}\{\|\tilde{\delta}_i(t)\|^2 + \|\tilde{\theta}_i(t)\|^2\}$, which follows $(\|e^g_1(t)\|^2 + \|e^g_2(t)\|^2)/(\|\tilde{\delta}_g(t)\|^2 + \|\tilde{\theta}_g(t)\|^2) \leq (N(\|e_1(t)\|^2 + \|e_2(t)\|^2))/(\|\tilde{\delta}(t)\|^2 + \|\tilde{\theta}(t)\|^2) = N\|\hat{e}(t)\|^2/\|\tilde{\omega}(t)\|^2$.

Referring to the first-order method, the time derivative of $\|\hat{e}(t)\|/\|\tilde{\omega}(t)\|$ is

$$\frac{d\|\hat{e}(t)\|}{dt\|\tilde{\omega}(t)\|} \leq \frac{\|\dot{\hat{e}}(t)\|}{\|\tilde{\omega}(t)\|} + \frac{\|\hat{e}(t)\|\|\dot{\tilde{\omega}}(t)\|}{\|\tilde{\omega}(t)\|^2}, \qquad (49)$$

where $\|\dot{\tilde{\omega}}(t)\|$ has

$$
\begin{aligned}
\|\dot{\tilde{\omega}}(t)\| &= \left\| \begin{bmatrix} \Upsilon & 0 \\ 0 & \Upsilon \end{bmatrix} \begin{bmatrix} L_d^T \theta(t) \\ -\varphi L_d^T L_d^T(\delta(t) + e_1(t) - \theta(t) - e_2(t)) \end{bmatrix} \right\| \\
&\leq \left\| \begin{bmatrix} 0 & 1 \\ 0 & 0 \end{bmatrix} \tilde{\omega}(t) \right\| + \left\| \begin{bmatrix} 0 & 0 \\ \varphi \Upsilon L_d^T \Upsilon^{-1} & \varphi \Upsilon L_d^T \Upsilon^{-1} \end{bmatrix} (\tilde{\omega} + I_2 \otimes (\Upsilon L_d^T)\hat{e}(t)) \right\| \\
&\leq \left(1 + \sqrt{2\varphi^2} \|\Upsilon L_d^T \Upsilon^{-1}\| \right)\|\tilde{\omega}(t)\| + \sqrt{2\varphi^2} \|\Upsilon L_d^T \Upsilon^{-1}\|)\|\Upsilon L_d^T\|\|\hat{e}(t)\| \\
&\leq \left(1 + \sqrt{2\varphi^2} \|\Upsilon L_d^T\| \right)\|\Upsilon^{-1}\|(\|\tilde{\omega}(t)\| + \|\Upsilon L_d^T\|\|\hat{e}(t)\|),
\end{aligned}
\qquad (50)
$$

and $\|\dot{\hat{e}}(t)\| = \|\dot{\omega}(t)\|$ is

$$
\begin{aligned}
\|\dot{\hat{e}}(t)\| = \|\dot{\omega}(t)\| &= \left\| \begin{bmatrix} \theta(t) \\ \varphi L_d^T(\delta(t) + e_1(t)) + \varphi L_d^T(\theta(t) + e_2(t)) \end{bmatrix} \right\| \\
&\leq \left(1 + \sqrt{2\varphi^2} \right)\|\Upsilon^{-1}\|(\|\tilde{\omega}(t)\| + \|\Upsilon L_d^T\|\|\hat{e}(t)\|).
\end{aligned}
\qquad (51)
$$

Combining (50) and (51), (49) is rearranged into

$$
\begin{aligned}
\frac{d\|\hat{e}(t)\|}{dt\|\tilde{\omega}(t)\|} &\leq \left(1 + \sqrt{2\varphi^2} \right) \frac{\|\tilde{\omega}(t)\| + \|\Upsilon L_d^T\|\|e(t)\|}{\|\Upsilon\|\|\tilde{\omega}(t)\|} \\
&\quad + \|\hat{e}(t)\|\left(1 + \sqrt{2\varphi^2} \|\Upsilon L_d^T\|\right)\frac{\|\tilde{\omega}(t)\| + \|\Upsilon L_d^T\|\|\hat{e}(t)\|}{\|\Upsilon\|\|\tilde{\omega}(t)\|^2} \\
&\leq \|\Upsilon^{-1}\|(\chi + \sqrt{2}\varphi)\left(1 + \frac{\|\Upsilon L_d^T\|\|\hat{e}(t)\|}{\|\tilde{\omega}(t)\|}\right)^2,
\end{aligned}
\qquad (52)
$$

where $\chi = \max\{1, 1/\|\Upsilon L_d^T\|\}$.

Additionally, define

$$
\begin{aligned}
\Xi &= \|\Upsilon^{-1}\|\left(1 + \sqrt{2\varphi^2}\right), \\
\Phi &= \frac{d\|\hat{e}(t)\|}{dt\|\tilde{\omega}(t)\|},
\end{aligned}
\qquad (53)
$$

for which, $\dot{\Phi} \leq \Xi(1 + \|\Upsilon L_d^T\|\Phi)^2$. Here, Φ satisfies the bound $\Phi \leq \phi(t, \phi_0)$, where $\phi(t, \phi_0)$ is the solution of $\dot{\phi}(t, \phi_0) = \Xi(1 + \|\Upsilon L_d^T\|)^2$, $\phi(0, \phi_0) = \phi_0$. Using $\tilde{\tau}_g$ to denote the time that $\phi(t, \phi_0)$ grows from 0 to $2\sigma k \mu_{\min}/((k_1 + \nu)\varphi \|\Upsilon L_d^T\|)$, we get $d\phi/(1 + \|\Upsilon L_d^T\|\phi)^2 \Xi = dt$.

Consequently, $\hat{\tau}_g$ is longer than $\tilde{\tau}_g$ that satisfies

$$\frac{\phi(\tilde{\tau}_g, 0)}{1 + \|\Upsilon L_d^T\|\phi(\tilde{\tau}_g, 0)} = \tilde{\tau}_g \Xi, \qquad (54)$$

where $\phi(\tilde{\tau}_g, 0) = ((2\sigma k \mu_{\min})/(\sqrt{N}(k_1 + \nu)))\gamma \|\Upsilon L_d^T\|$.

Thus, $\tilde{\tau}_g = (2\sigma k \mu_{\min})/(\|\Xi\|\|\Upsilon L_d^T\|(\gamma\sqrt{N}(k_1 + \nu) + 2\sigma k \mu_{\min}))$. From $\tau_g > \hat{\tau}_g > \tilde{\tau}_g$, we conclude that in system (25), there exists at least one agent $g \in \mathcal{N}$ that the next interevent interval is strictly positive under event-triggered condition (40). The proof is complete. □

5. Simulation Examples

Considering an MAS (7) consisting of six agents, the desired distances between two adjacent agents are set to $d = [\pi/8, t\pi/2n, q3\pi/8h_{\pi/2x}, 7\pi/3C, ;\pi/6]^T$, and the initial values of the MAS are randomly generated to satisfy (8). In each case, we apply the same initial settings, i.e., same angular positions and same admissible circle formations. Additionally, the unique normalized positive left eigenvector
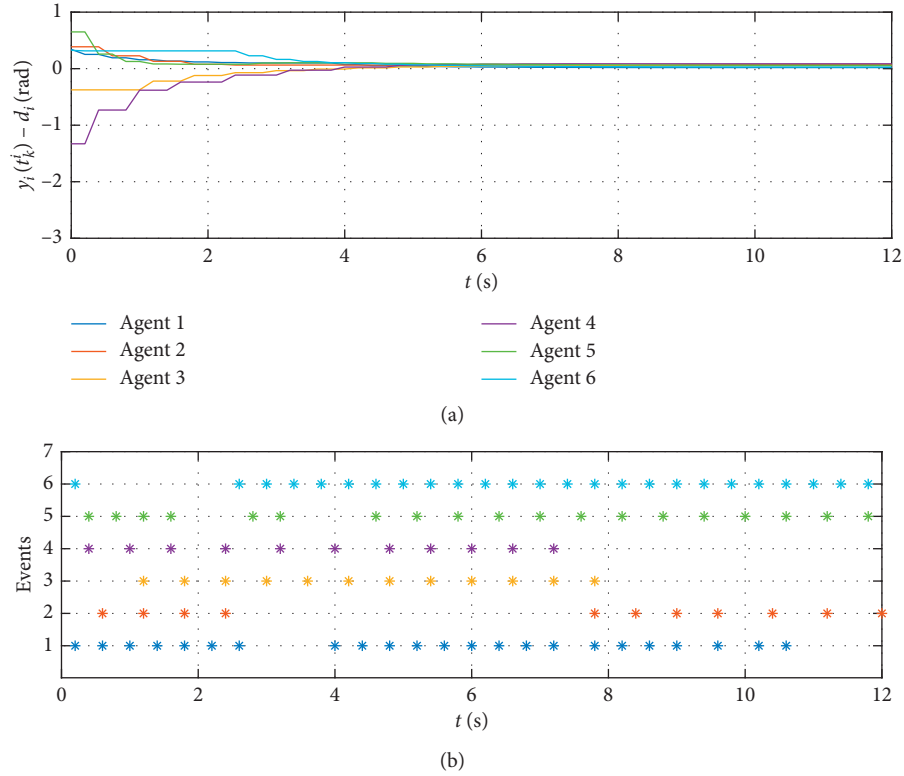
(a)

(b)

FIGURE 2: Simulation results of circle formation control for first-order MASs. (a) The evolution of $y_i(t_k^i) - d_i$ for $i = 1, 2, \ldots, N$ when $h = 0.2$ s. (b) The sequence of event-triggered times for $i = 1, 2, \ldots, N$ when $h = 0.2$ s.
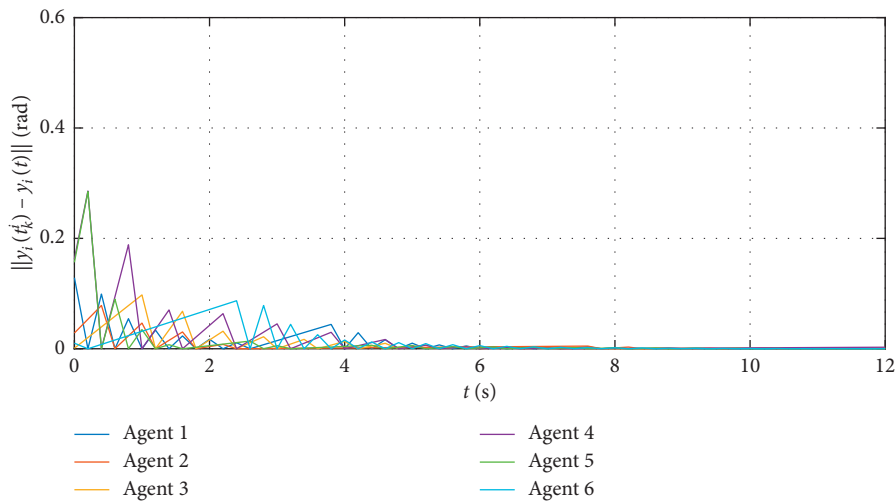

FIGURE 3: The evolution of $\|y_i(t_k^i) - y_i(t)\|$ for $i = 1, 2, \ldots, N$ when $h = 0.2$ s.

of L_d^T with respect to eigenvalue 0 is $\xi = [0.0625\, 0.\, 0.25\, 0.1875\, 0.25\, 0.1667\, 0.0833]^T$. In order to show advantages of the event-triggered control strategy, it is worth pointing out that the event detection of all those simulations is implemented in a sampled-data fashion, which is proved to be effective, and there is at least one trigger interval with a positive bound. Therefore, the sampling periods h in real-time control is chosen as 0.2 s.

5.1. Simulation of the First-Order MAS. By the permitted range $0 < \sigma < 1$, we set $\sigma = 0.9$ to ensure condition (15) holds in real-time control. Simulation results are shown in Figures 2 and 3. Figure 2(a) shows the evolution difference between the event-triggered angular distance and the expected counterpart, while Figure 2(b) reveals the event sequence of each agent. Figure 3 illustrates the fluttering of the measurement error $\|y_i(t_k^i) - y_i(t)\|$.
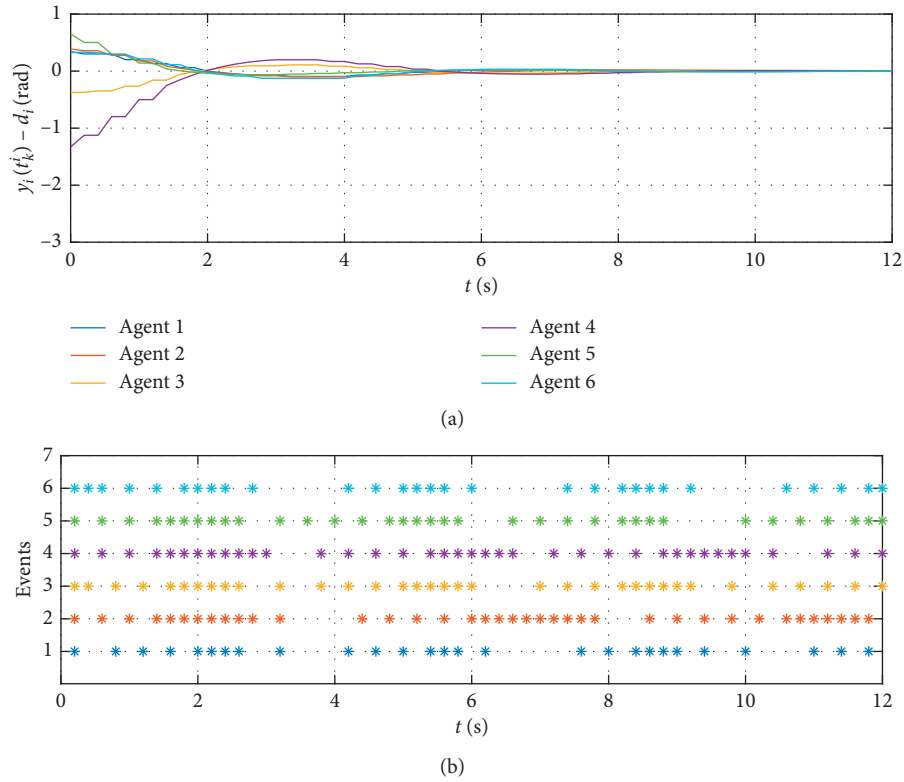
FIGURE 4: Simulation results of circle formation for second-order MASs. (a) The evolution of $y_i(t_k^i) - d_i$ for $i = 1, 2, \ldots, N$ when $h = 0.2$ s. (b) The sequence of event-triggered times for $i = 1, 2, \ldots, N$ when $h = 0.2$ s.
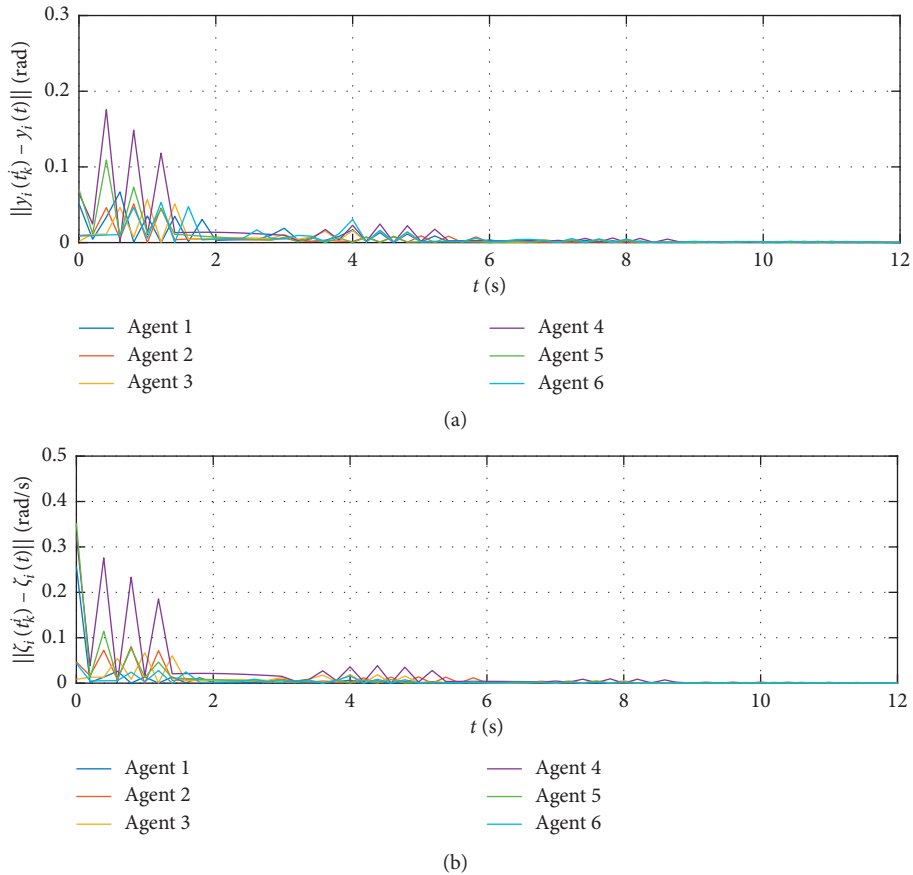

FIGURE 5: Simulation results of the fluttering of the measurement error. (a) The evolution of $\|y_i(t_k^i) - y_i(t)\|$ for $i = 1, 2, \ldots, N$ when $h = 0.2$ s. (b) The evolution of $\|\zeta_i(t_k^i) - \zeta_i(t)\|$ for $i = 1, 2, \ldots, N$ when $h = 0.2$ s.

We can see from the simulation results that the desired circle formation can be asymptotically achieved by the proposed control law (10) in distributed MASs. We also calculate the average interevent time of all mobile agents $h_{avg} = 0.6059$ from Figure 2, and the result indicates that our method can reduce the amount of control update for first-order MASs.

5.2. Simulation of the Second-Order MAS. We choose coefficients $\sigma = 0.9$, $\varphi = 1.2$, $k_2 = 0.5$, $k_1 = 2$, $k = 0.8$, $o = 2$, and $\nu = 2$ to ensure condition (40) holds in real-time control. Simulation results are shown in Figures 4 and 5. Figure 4(a) shows the evolution difference between the event-triggered angular distance and the expected counterpart, while Figure 4(b) reveals event sequence of each agent. Figure 5 shows the fluttering of the measurement error $\|y_i(t_k^i) - y_i(t)\|$, $\|\zeta_i(t_k^i) - \zeta_i(t)\|$.

We observe from the simulation results that the desired circle formation can also be asymptotically achieved under the proposed control law (27). Similarly, we calculate the average interevent time of all mobile agents $h_{avg} = 0.3545$ from Figure 4. We conclude that our proposed method has the advantages of reducing the amount of control update for the second-order MASs.

To sum up, compared with traditional time-planning controls in the same simulation environment, the event-triggered control-based formation control strategies proposed in this paper show the effectiveness for both first- and second-order MASs. For the second-order MAS, the average interevent time of all mobile agents is less than the first-order MAS case due to its more complicated modeling. However, from an application point of view, the proposed control strategy for second-order MASs is much more accurate than first-order MASs.

6. Conclusion

This paper investigated the circle formation control problem for both first- and second-order MASs under unbalanced directed networks with limited resource constraints. We first designed the observer-based event-triggered algorithm to reduce dependence on resources, in which, when the value of the event-triggered condition exceeds zero, the agent's controller will update its states simultaneously. Moreover, it is a fundamental and practical aspect to observe neighbor information on a regular or better basis continuously. Then, we proved that if there is a spanning tree in the underlying graph, the MASs can achieve the desired circle formation by the proposed control laws, and there is at least one agent whose the next interevent interval is strictly positive. At last, we gave numerical simulation examples to illustrate that the proposed event-triggered circle formation control strategies are effective for both first- and second-order MASs. For future work, we will extend our research to more practical operations, e.g., considering the effect of time delays in communication networks, input saturation constraints, and weak links.

Data Availability

The data used to support the findings of this study are available from the corresponding author upon request.

Conflicts of Interest

The authors declare that there are no conflicts of interest regarding the publication of this paper.

References

[1] A. Macwan, J. Vilela, G. Nejat, and B. Benhabib, "Multi-robot deployment for wilderness search and rescue," *International Journal of Robotics and Automation*, vol. 31, no. 1, 2016.

[2] K. Kim, H. Kim, and H. Myung, "Bio-inspired robot swarm control algorithm for dynamic environment monitoring," *Advances in Robotics Research*, vol. 2, no. 1, pp. 1–11, 2018.

[3] A.-Q. Hoang and M.-T. Pham, "Swarm intelligence-based approach for macroscopic scale odor source localization using multi-robot system," in *Advances in Information and Communication Technology*, pp. 593–602, Springer, Berlin, Germany, 2016.

[4] T. Yang, Z. Meng, D. V. Dimarogonas, and K. H. Johansson, "Global consensus for discrete-time multi-agent systems with input saturation constraints," *Automatica*, vol. 50, no. 2, pp. 499–506, 2014.

[5] G. Nava-Antonio, G. Fernández-Anaya, E. Hernández-Martínez, J.-J. Flores-Godoy, and E. D. Ferreira-Vázquez, "Consensus of multiagent systems described by various noninteger derivatives," *Complexity*, vol. 2019, Article ID 3297410, 14 pages, 2019.

[6] B. Yang, X. Wang, J.-a. Fang, and Y. Xu, "The impact of coupling function on finite-time synchronization dynamics of multi-weighted complex networks with switching topology," *Complexity*, vol. 2019, Article ID 7276152, 15 pages, 2019.

[7] M. Villani, L. Sani, R. Pecori et al., "An iterative information-theoretic approach to the detection of structures in complex systems," *Complexity*, vol. 2018, Article ID 3687839, 15 pages, 2018.

[8] C. Wang, G. Xie, and M. Cao, "Forming circle formations of anonymous mobile agents with order preservation," *IEEE Transactions on Automatic Control*, vol. 58, no. 12, pp. 3248–3254, 2013.

[9] K.-K. Oh, M.-C. Park, and H.-S. Ahn, "A survey of multi-agent formation control," *Automatica*, vol. 53, pp. 424–440, 2015.

[10] X. Ge, Q. Han, and X. Zhang, "Achieving cluster formation of multi-agent systems under aperiodic sampling and communication delays," *IEEE Transactions on Industrial Electronics*, vol. 65, no. 4, pp. 3417–3426, 2017.

[11] Z. Bu, Z. Wu, J. Cao, and Y. Jiang, "Local community mining on distributed and dynamic networks from a multiagent

perspective," *IEEE Transactions on Cybernetics*, vol. 46, no. 4, pp. 986–999, 2017.

[12] D. Tian, J. Zhou, and Z. Sheng, "An adaptive fusion strategy for distributed information estimation over cooperative multi-agent networks," *IEEE Transactions on Information Theory*, vol. 63, no. 5, pp. 3076–3091, 2017.

[13] G. Wen, H.-T. Zhang, W. Yu, Z. Zuo, and Y. Zhao, "Coordination tracking of multi-agent dynamical systems with general linear node dynamics," *International Journal of Robust and Nonlinear Control*, vol. 27, no. 9, pp. 1526–1546, 2017.

[14] R. Olfati-Saber and R. M. Murray, "Consensus problems in networks of agents with switching topology and time-delays," *IEEE Transactions on Automatic Control*, vol. 49, no. 9, pp. 1520–1533, 2004.

[15] W. Xie, B. Ma, T. Fernando, and H. C. Iu, "A new formation control of multiple underactuated surface vessels," *International Journal of Control*, vol. 91, no. 10, pp. 1–12, 2017.

[16] P. Tabuada, "Event-triggered real-time scheduling of stabilizing control tasks," *IEEE Transactions on Automatic Control*, vol. 52, no. 9, pp. 1680–1685, 2007.

[17] G. S. Seyboth, D. V. Dimarogonas, and K. H. Johansson, "Event-based broadcasting for multi-agent average consensus," *Automatica*, vol. 49, no. 1, pp. 245–252, 2013.

[18] X. Ge and Q.-L. Han, "Distributed formation control of networked multi-agent systems using a dynamic event-triggered communication mechanism," *IEEE Transactions on Industrial Electronics*, vol. 64, no. 10, pp. 8118–8127, 2017.

[19] Y. Liu and X. Hou, "Event-triggered consensus control for leader-following multiagent systems using output feedback," *Complexity*, vol. 2018, Article ID 6342683, 9 pages, 2018.

[20] D. V. Dimarogonas, E. Frazzoli, and K. H. Johansson, "Distributed event-triggered control for multi-agent systems," *IEEE Transactions on Automatic Control*, vol. 57, no. 5, pp. 1291–1297, 2011.

[21] P. Xu, H. Zhao, G. Xie, J. Tao, and M. Xu, "Pull-based distributed event-triggered circle formation control for multi-agent systems with directed topologies," *Applied Sciences*, vol. 9, no. 23, p. 4995, 2019.

[22] J. Wen, C. Wang, and G. Xie, "Asynchronous distributed event-triggered circle formation of multi-agent systems," *Neurocomputing*, vol. 295, pp. 118–126, 2018.

[23] J. Wen, P. Xu, C. Wang, G. Xie, and Y. Gao, "Distributed event-triggered circle formation control for multi-agent systems with limited communication bandwidth," *Neurocomputing*, vol. 358, pp. 211–221, 2019.

[24] P. Xu, J. Wen, C. Wang, and G. Xie, "Distributed circle formation control over directed networks with communication constraints," *IFAC-PapersOnLine*, vol. 52, no. 3, pp. 108–113, 2019.

[25] K. H. Johansson, M. Egerstedt, J. Lygeros, and S. Sastry, "On the regularization of zeno hybrid automata," *Systems & Control Letters*, vol. 38, no. 3, pp. 141–150, 1999.

[26] M. Heymann, F. Lin, G. Meyer, and S. Resmerita, "Control synthesis for a class of hybrid systems subject to configuration-based safety constraints," *Hybrid and Real-Time Systems*, vol. 50, no. 3, pp. 376–390, 2005.

[27] C. Nowzari, *Distributed Event-Triggered Coordination for Average Consensus on Weight-Balanced Digraphs*, Pergamon Press, Oxford, UK, 2016.

[28] S. Zaman, W. Slany, and G. Steinbauer, "Ros-based mapping, localization and autonomous navigation using a pioneer 3-dx robot and their relevant issues," in *Proceedings of the Saudi International Electronics, Communications and Photonics Conference (SIECPC)*, pp. 1–5, Riyadh, Saudi Arabia, April 2011.

[29] M. Yu, H. Wang, G. Xie, and K. Jin, "Event-triggered circle formation control for second-order-agent system," *Neurocomputing*, vol. 275, no. 31, pp. 462–469, 2017.

[30] W. Ren and R. W. Beard, "Consensus seeking in multiagent systems under dynamically changing interaction topologies," *IEEE Transactions on Automatic Control*, vol. 50, no. 5, pp. 655–661, 2005.